

****TITLE****
*ASP Conference Series, Vol. **VOLUME**, **YEAR OF PUBLICATION***
****NAMES OF EDITORS****

Diffusive Nuclear Burning in Neutron Star Envelopes

Philip Chang

Department of Physics, Broida Hall, University of California, Santa Barbara, CA 93106; pchang@physics.ucsb.edu

Lars Bildsten

Kavli Institute for Theoretical Physics and Department of Physics, Kohn Hall, University of California, Santa Barbara, CA 93106; bildsten@kitp.ucsb.edu

Abstract. We present a new mode of hydrogen burning on neutron stars (NSs) called diffusive nuclear burning (DNB). In DNB, the burning occurs in the exponentially suppressed tail of hydrogen that extends to the hotter regions of the envelope where protons are readily captured. Diffusive nuclear burning changes the compositional structure of the envelope on timescales $\sim 10^{2-4}$ yrs, much shorter than otherwise expected. This mechanism is applicable to the physics of young pulsars, millisecond radio pulsars (MSPs) and quiescent low mass X-ray binaries (LMXBs).

1. Introduction

The composition of NS envelopes affects their cooling (Potekhin, Chabrier & Yakovlev 1997) and thermal radiation (Romani 1987). The amount of material needed to change the spectral profile of the thermal radiation from the surface of a NS is miniscule ($\sim 10^{-20} M_{\odot}$). Such a small amount of contamination could easily be produced from spallation (Bildsten, Salpeter & Wasserman 1992) of fallback material (Woosley & Weaver 1995) soon after a supernova explosion.

Recent X-ray observations of the thermal spectrum from young radio pulsars have yielded tantalizing clues of their photospheric makeup (see Pavlov, Zavlin & Sanwal 2002 for a review). The thermal emission from young NSs can be fit with two models: magnetic hydrogen atmospheres or blackbody atmospheres. Both atmospheres fit the thermal spectra equally well, however they yield different effective temperatures and different solid angles for the emission area. The model which yields a more reasonable radius for the NS at the preferred distance is then taken as the favored model (Pavlov et al. 2002). For radio pulsars younger than $\sim 10^{4-5}$ yrs (e.g. Vela), the radius is reasonable for a magnetic hydrogen atmosphere model (Pavlov et al. 2001). For pulsars older than $\sim 10^{4-5}$ yrs (e.g. PSR B0656+14), a blackbody model is favored (see Pavlov et al. 2002 and references therein). This suggests a possible evolution of hydrogen to more blackbody like elements on a timescale of 10^{4-5} yrs, and these indications have motivated our work.

At the photosphere, the local temperature ($T \sim 10^6$ K) and density ($\rho \sim 1 \text{ g cm}^{-3}$) are too low to allow any significant nuclear evolution over 10^{4-5} yrs. However at a depth 1 m underneath the photosphere, the temperature is roughly two orders of magnitude greater ($T \sim 10^8$ K). Consider a NS envelope of hydrogen on carbon (we use C here as our fiducial proton capturing nucleus, results for other nuclei are in Chang & Bildsten 2003; CB03 hereafter) as shown in Figure 1. In diffusive equilibrium, the separation between the hydrogen and carbon is not strict. Rather a diffusive tail of hydrogen penetrates deep into the carbon layer. Protons easily reach a depth where the temperature is sufficiently high for rapid capture onto C. Since the hydrogen's diffusive tail is exponen-

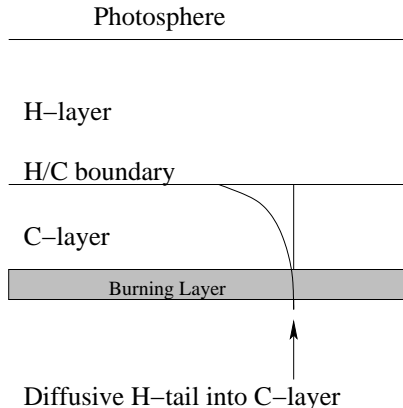


Figure 1. Schematic of a H/C envelope in diffusive equilibrium. The diffusive tail of hydrogen extends deep into the carbon, reaching temperatures where the hydrogen rapidly captures onto carbon, forcing depletion of the hydrogen layer as protons diffuse down to the burning layer.

tially suppressed, there will be a region where proton captures are peaked, which we call the burning layer. The consumption of the hydrogen by burning will drive the diffusive tail out of equilibrium, which sets up a diffusive current of hydrogen that flows down from the hydrogen layer into the burning layer. We refer to this burning mechanism (first mentioned by Chui & Salpeter 1964 and initially calculated by Rosen 1968) as diffusive nuclear burning (DNB; CB03). Over time, given that there is no interstellar accretion or other processes to refresh the hydrogen layer, the H is depleted.

This scenario presents several competing timescales. The first is the proton capture timescale in the burning layer, τ_{nuc} . The second is the time it takes protons to diffuse into the burning layer, τ_{diff} . In the case where $\tau_{\text{diff}} \ll \tau_{\text{nuc}}$, the diffusive tail is always in equilibrium. In the opposite limit, the diffusive tail is modified by the burning. For simplicity we will only discuss the first case here.

The equilibrium structure of the diffusive tail is calculated from hydrostatic balance for each ion,

$$\frac{dP_i}{dr} = -n_i (A_i m_p g - Z_i e E), \quad (1)$$

$$\frac{dP_e}{dr} = -n_e (m_e g + e E), \quad (2)$$

where P_i , n_i , A_i , Z_i are the pressure, number density, atomic number and charge of the i 'th ion species and E is the upward pointing electric field found by demanding charge neutrality, $n_e = \sum n_i Z_i$. The thermal structure is determined from the constant flux equation,

$$\frac{dT}{dr} = -\frac{3\kappa\rho}{16T^3} T_e^4, \quad (3)$$

where κ is the opacity and T_e is the effective temperature. Given appropriate microphysics, the equilibrium thermal and compositional structure can be calculated (see CB03 for additional details). The microphysics we have chosen in this paper are valid for the non-magnetic case, $B < 10^9$ G.

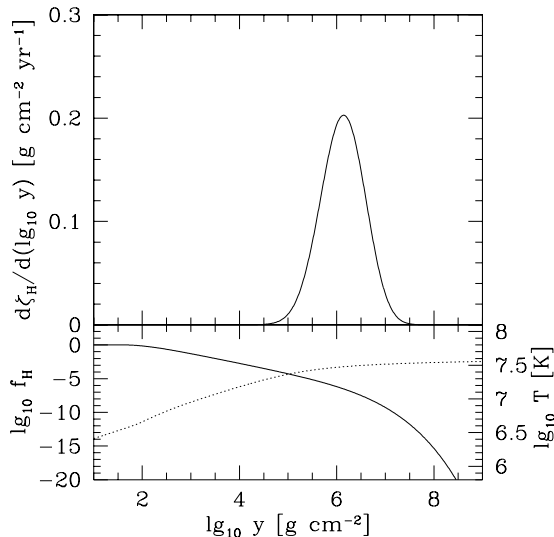


Figure 2. Differential hydrogen column burning rate taking into account p-p capture and p + C capture. The bottom graph shows the number fraction (solid line) and temperature (dotted line). This model has $y_H = 100 \text{ g cm}^{-2}$ and $T_e = 8 \times 10^5 \text{ K}$. The integrated burning rate for this model is $y_H/\tau_{\text{col}} = 0.24 \text{ g cm}^{-2} \text{ yr}^{-1}$, giving $\tau_{\text{col}} = 417 \text{ yrs}$.

The local hydrogen burning rate is $m_p n_H / \tau_{\text{nuc}}$, hence the total hydrogen burning rate per area on a NS, ζ_H , is

$$\zeta_H = \frac{y_H}{\tau_{\text{col}}} = \int \frac{n_H m_p}{\tau_H(n_H, n_C, T)} dz, \quad (4)$$

where $y_H = \int m_p n_H dz$ is the integrated column of hydrogen and τ_{col} is the characteristic burning time for that column. In Figure 2, we show the equilibrium structure for a fiducial NS model with $T_e = 8 \times 10^5 \text{ K}$ and the total burning rate per log column, $y = P/g$. The Gaussian peak in the burning rate traces out the burning zone which is centered around a column of $y \approx 10^6 \text{ g cm}^{-2}$, which is about 20 cm below where most of the H resides.

We relate the burning rate per column into a total mass burning rate $\dot{M}_{\text{DNB}} = 4\pi R_*^2 \zeta_H$. In Figure 3, we plot the characteristic burning time τ_{col} and associated \dot{M}_{DNB} as a function of the total hydrogen column, y_H . For a given envelope with an initial column of hydrogen at a fixed core temperature, the evolution follows the curve up to the photosphere at $y_H \sim 1 \text{ g cm}^{-2}$. Because the evolution follows a simple power law, the lifetime for any given envelope is completely determined by the characteristic burning time, τ_{col} , at the photosphere. The curve for a central temperature of $T_c = 5 \times 10^7 \text{ K}$ is cut off at large columns since the energy release from proton captures is comparable to the flux leaving the envelope. Hence our assumption of constant flux is violated. What is also notable about Figure 3 is that the curves follow a power law dependence which we derive in CB03.

Future directions for DNB are including the microphysics for magnetic NSs, calculating DNB without the constraint $\tau_{\text{diff}} \ll \tau_{\text{nuc}}$ and allowing for an intervening helium layer. DNB allows for young neutron stars to have atmospheres other than hydrogen soon after birth. For instance, NSs with carbon, nitrogen or oxygen photospheres can

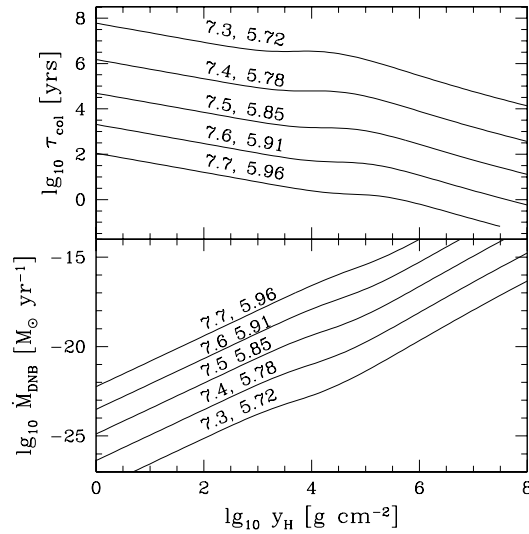


Figure 3. Characteristic burning time, τ_{col} , and total mass burning rate, \dot{M}_{DNB} for a NS radius of 10 km, as a function of y_H for different fixed core temperatures and an underlying carbon layer. For each model, we list the logarithmic core temperature and associated logarithmic effective temperature.

easily exist after burning off any initial H. DNB may help explain the recent observation of magnetic oxygen lines on 1E1207+56 (see De Luca’s review in this volume, also see Hailey & Mori 2002).

Acknowledgments. This research was supported by NASA via grant NAG 5-8658 and by the NSF under Grants PHY99-07949 and AST01-96422. L. B. is a Cottrell Scholar of the Research Corporation.

References

- Bildsten, L., Salpeter, E. E. & Wasserman, I. 1992, *ApJ*, 384, 143
 Chang, P. & Bildsten, L. 2003, to appear in *ApJ*, astro-ph/0210218
 Chiu, H. Y., Salpeter, E. E., 1964, *Phys.Rev.Lett*, 12, 413
 Hailey, C. J. & Mori, K. 2002, *ApJ*, 578, L133
 Pavlov, G. G., Zavlin, V. E., Sanwal, D., Burwitz, V., Garmire, G. P. 2001, *ApJ*, 552, L129
 Pavlov, G. G., Zavlin, V. E., & Sanwal, D. 2002, in *Proceedings of the 270. Heraeus Seminar on Neutron Stars, Pulsars and Supernova Remnants*, ed. W. Becker, H. Lesch and J. Trumper, astro-ph/0206024
 Potekhin, A. Y., Chabrier, G., & Yakovlev, D. G. 1997, *A&A*, 323, 415
 Potekhin, A. Y. & Yakovlev, D. G. 2001, *A&A*, 374, 213
 Romani, R. W. 1987, *ApJ*, 313, 718
 Rosen, L. C., 1968, *Ap&SS*, 1, 372
 Woosley, S. E. & Weaver, T. A. 1995, *ApJS*, 101, 181